The pathway to energy localization in nonlinear lattices.

Michel Peyrard

Ecole Normale Supérieure de Lyon, 46 allée d'Italie, 69364 Lyon Cedex 07, France

Abstract

Intrinsic localized modes have been shown to exist as exact solutions in nonlinear lattices [R.S. MacKay and S. Aubry, Nonlinearity **7** 1623 (1994)]. We investigate the mechanisms that can lead to their formation in a physical system. We show that they can emerge from a uniform energy distribution in several steps. First modulational instability can generate small breathers and then their interaction leads to the growth of the largest excitations. This mechanism, first investigated in simple one-dimensional lattices is shown to be valid in a multicomponent lattice as well as in a two-dimensional system. The signature of the discrete breathers in the dynamical structure factor of the lattice is determined and the consequences for their experimental detection are discussed. Finally some suggestions for indirect observations of the discrete breathers are presented.

1 Introduction

Intrinsic localized modes in nonlinear lattices, also called discrete breathers, are very interesting because they provide examples of localized excitations in homogeneous systems. Approximate solutions have been obtained for one-dimensional or multidimensional lattices [1–3] and a proof of existence of time-periodic, spatially localized, solutions, or breathers, has been given for a broad range of Hamiltonian coupled oscillators lattices [4,5]. However the existence of exact solutions is not a guarantee of their relevance in physical systems. They must be generated easily in a system and, if we want to observe them, they must have a particular signature that can be detected in experiments or have significant consequences in the physical properties of the system. The present paper discusses these questions in systems where the nonlinearity comes from an on-site potential, i.e. systems that would be described by a nonlinear Klein-Gordon equation in the continuum limit. The proof of existence shows that the discreteness of the lattice is crucial for the *existence* of intrinsic localized modes. We discuss here the role that it plays in their *formation*.

The organization of the paper is the following. Section 2 reviews our previous results on a simple one-dimensional lattice. Section 3 considers more complex systems. It starts from a review of recent results on a multicomponent lattice and then presents new results on a two-dimensional system. Section 4 discusses the signature of discrete breathers in experiments through the calculation of the structure factor of the lattice and the identification of its main features. Section 5 summarizes the paper and makes some suggestions on the possible observation of discrete breathers in a physical system.

2 Formation of discrete breathers in a simple one-dimensional lattice.

Discrete breathers are large amplitude nonlinear excitations and therefore they can only appear if one introduces enough energy into a lattice. At a microscopic scale in a homogeneous lattice, it is generally not possible to excite selectively a few sites and therefore the initial excitation is extended over the whole system. The energy can be introduced coherently, as a plane wave, or incoherently under the form of fluctuations. The first situation, which is the simplest, is nevertheless interesting because it provides some insight on the more realistic case of incoherent fluctuations which can come from a thermal bath. The localization of energy can be initiated by the modulational instability of the plane wave [6,7]. We discuss this initial stage first and then show how large amplitude breathers can be formed.

2.1 Modulational instability as a first step in breather generation.

Let us consider the simple case of a one-dimensional lattice described by the Hamiltonian

$$H = \sum_n \frac{p_n^2}{2} + \frac{1}{2}K(u_{n+1} - u_n)^2 + V(u_n) \tag{1}$$

with the on-site potential

$$V(u) = \frac{\omega_0^2 u^2}{2} - \frac{\alpha u^3}{3} - \frac{\beta u^4}{4}\,, \tag{2}$$

where u_n is the displacement of the n^{th} particle, p_n its momentum, α and β measure the nonlinearity of the potential and ω_0^2 determines the relative weight of the on-site potential with respect to the coupling characterized by

K. In order to analyze the stability of a plane wave, we can look for solutions of the equations of motions that derive from Hamiltonian (1) under the form

$$u_n(t) = F_{1,n}(t)e^{-i\omega_0 t} + F_{3,n}(t)e^{-3i\omega_0 t} + c.c. \tag{3}$$

for a symmetrical potential ($\alpha = 0$), and

$$u_n(t) = F_{1,n}(t)e^{-i\omega_0 t} + F_{0,n}(t) + F_{2,n}(t)e^{-2i\omega_0 t} + c.c. \tag{4}$$

for a non-symmetrical potential ($\alpha \neq 0$, $\beta = 0$).

Assuming a slowly varying envelope $|\dot{F}_{i,n}(t)| \ll \omega_0 |F_{i,n}(t)|$ and *a highly discrete lattice* $\omega_0^2 \gg 4K$, one gets a discrete NLS equation for the envelope

$$2i\omega_0 \dot{F}_{1,n} + K(F_{1,n+1} + F_{1,n-1} - 2F_{1,n}) + \gamma |F_{1,n}|^2 F_{1,n} = 0 \; . \tag{5}$$

This equation can be used to investigate the stability of a coherently modulated wave defined by the initial condition

$$\begin{aligned} u_n(0) &= (2\phi_0 + 4b_0 \cos nQ) \cos nq \\ \dot{u}_n(0) &= (2\phi_0 + 4b_0 \cos nQ)\omega \sin nq \; . \end{aligned} \tag{6}$$

The short term evolution of such an excitation is very well described by a linear stability analysis which gives the dispersion relation $\Omega(Q)$, provided the harmonics created by the nonlinearity are included. For instance, in a symmetrical potential for which the equations of motion contain a cubic term, one must not only consider the $\cos nq$ term but also a small contribution in $\cos^3 nq$ which introduces factors of the form $\cos 2nq \cos nq$, i.e. the nonlinear term can be viewed as a modulation of the $\cos nq$ plane wave with a wavevector $Q = 2q$. When such nonlinear terms are considered in addition to the applied modulation, numerical simulations show that the first stage of the time evolution of an initial condition such as (6) is accurately predicted by the linear stability analysis [7]. The long term evolution is however more complicated because higher harmonics start to play a role and the growth of some components due to their instability requires an analysis that involves a mode coupling approach. For the purpose of the generation of discrete breathers from a coherently modulated wave, the basic conclusion of these studies is that modulational instability is much more likely to occur in a lattice than in the continuum limit for two reasons: first the linear stability study leads to a broader range of instability in the parameter space (q, Q) than for a continuum medium, and second one must take into account the folding of the Brillouin zone. In a discrete medium, only the wavevectors belonging to the first Brillouin zone ($|q| < \pi$) are meaningful. Any wave with a larger wavevector can also be described by a wave with a wavevector in the first Brillouin

zone. It means that combination wavevectors such as $3q$, $4q$, $5q$, $2q+Q$, ... which appear due to the nonlinearities, must be interpreted modulo 2π. As a consequence these terms, that would lead to large wavevectors that belong to the domain of stability in a continuous medium, may in fact behave in the discrete lattice as small wavevector modulations, that belong to the instability region.

The case of a randomly modulated wave is more interesting because it mimics the effects of thermal fluctuations that would always be superimposed in a real system to a plane wave excitation due for instance to the effect of an electromagnetic wave on a ionic crystal. Figure 1 shows the spectrum of the excitation generated by a noisy wave

$$u_n(0) = (2\phi_0 + \Gamma(n)) \cos nq, \quad \Gamma(n) \text{ Gaussian noise .} \tag{7}$$

The initial spectrum was almost a sharp peak because the noise was extremely small. Then it develops side bands due to modulational instability of some of the components. Figure 1 shows that the prediction of the modulational instability in the discrete lattice that one can derive from Eq. (5) is very accurate.

2.2 The growth of large amplitude breathers.

Modulational instability is however only the first step in the formation of discrete breathers. This is illustrated in Fig. 2 which shows the long term evolution (15000 periods of the lowest phonon $T_0 = 2\pi/\omega_0$) of the energy density in the lattice, for an initial noisy wave as above.

One can notice three main stages in the time evolution. The first one is the modulation of the energy density which was initially uniform. It is fast and leads to energy density maxima which are almost equally spaced. They correspond to small breathers, and their mean separation can be estimated with the linear stability analysis described above. It is determined by the fastest growing modulation of the initial wave. But modulational instability cannot lead to very large breathers because the typical energy of a breather is given by the product of the mean energy density $\overline{E_n}$ by the preferred modulation length. Figure 2 shows that larger breathers can emerge in a second stage which takes a longer time. They result from the collisions of the small breathers generated in the first stage. When two of them collide they do not behave as exact solitons as they would in a continuum medium. In most of the cases, the largest of the two takes some energy from the smallest. After the multiple collisions that occur during the second stage, a few large breathers have collected most of the energy of the initial plane wave. Then, during the third stage the distribution

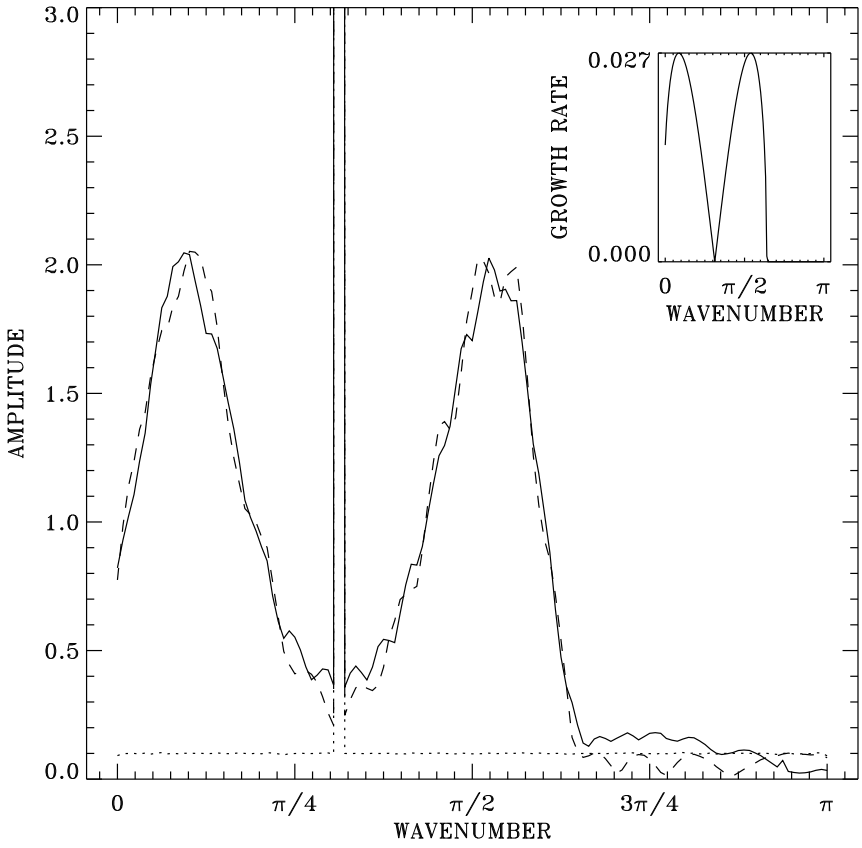

Fig. 1. Fourier spectrum of the time evolution at $t = 150$ of a noisy plane wave in a discrete lattice. The dotted line shows the spectrum of the initial condition. The random modulation is so small that the initial spectrum appears only as a sharp peak. At a later time, the spectrum (full line) shows the formation of two side bands coming from to the growth of the random fluctuations due to modulational instability. The inset shows the growth rate of the modulated waves and the dashed line indicated the shape of the side bands predicted by the modulational instability study of the initial condition. This figure has been generated by averaging over a set of 1000 initial conditions, for parameters $\alpha = 0$, $\beta = 0.5$, $K = 2$, $\phi_0 = 0.6$, $\omega_0^2 = 100$ and a gaussian noise of variance 1 and amplitude 0.01. (from Ref. [7])

of energy density in the lattice stays almost stationary with sharp maxima at the positions of the large breathers which do not move along the lattice. This is because as they grow the breathers also become narrower so that their width falls down to a few lattice spacing. At this stage, the breathers feel the discreteness very strongly and stay pinned to the lattice. This effect is very similar to the pinning of kinks or dislocations by the Peierls barrier, although, for breathers that have an internal oscillation, a Peierls potential depending only on the position of the breather cannot be defined [8]. The third stage is then extremely stable and extremely long simulations are required to see the decay of some of the highly localized breathers due to their interaction

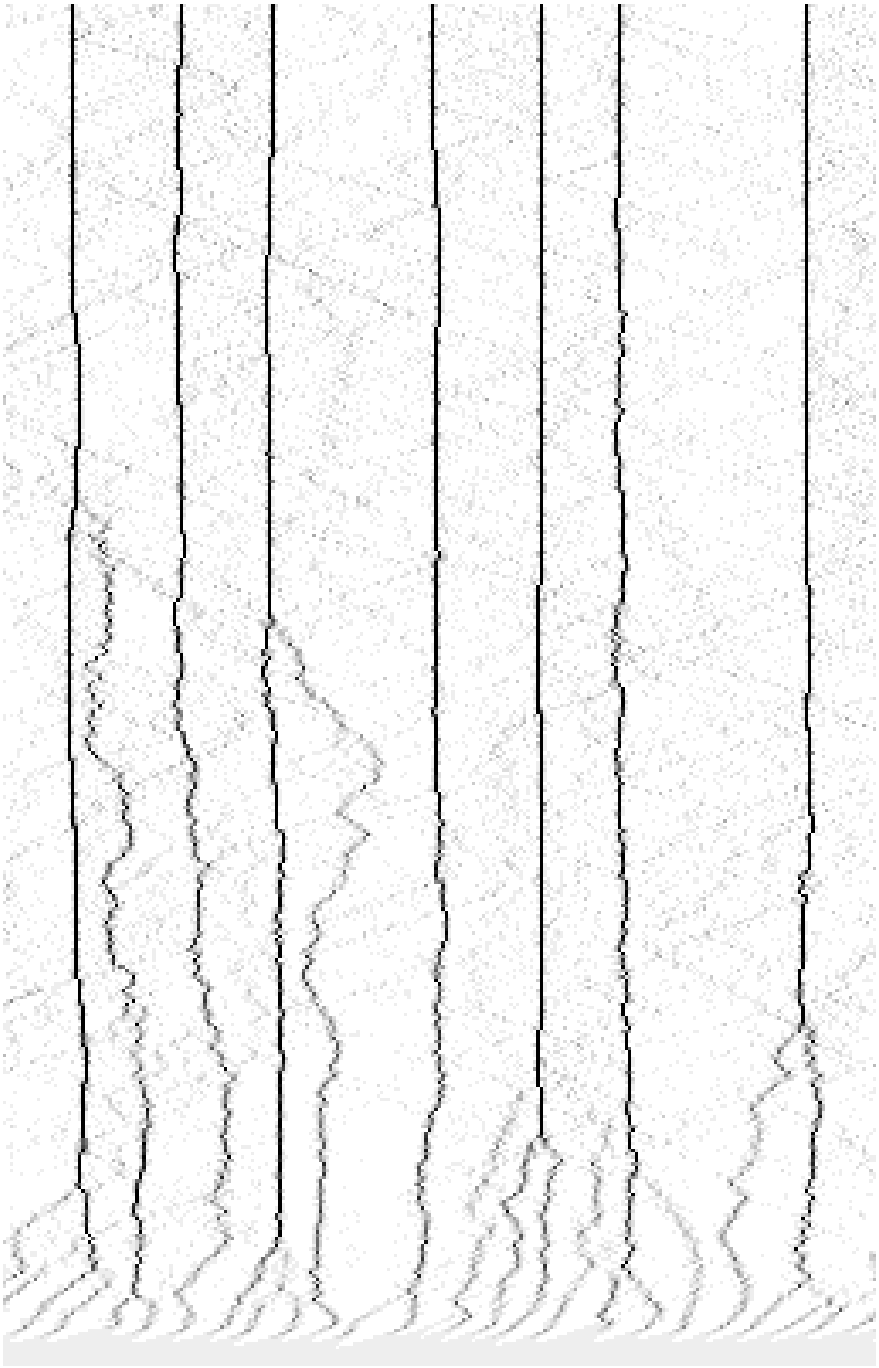

Fig. 2. Long term evolution of the energy density along the chain for an initial condition corresponding to a noisy wave given by Eq. (7). The horizontal axis indicates the position along the chain and the vertical axis corresponds to time, going upward. The energy density at site n is shown by a grey scale from $E_n = 0$ (white) to the maximum E_n recorded during the simulation (black).

with the background of small amplitude excitations that remain from the first stage [9]. In a system in contact with a thermal bath, after such a decay, another breather may emerge elsewhere from the fluctuations. As a result, if one observes the system in contact with the bath over a time interval which is extremely long in comparison with the phonon periods, energy equipartition is found, but, on time scales of the order of 10000 phonon periods one can detect a localization of most of the energy in small regions of the lattice.

An analytical study of the growth of breathers through collisions is difficult because it involves small energy exchanges and we do not have an exact analytical expressions of the discrete breathers. A numerical study can confirm the existence of such a growth mechanism and give some quantitative data on this process. As breathers are modes with an internal degree of freedom and because they move in a discrete medium, the output of their collisions depends on their relative phases and on the exact location of the collision point with respect to the lattice sites. To get meaningful results concerning the spontaneous localization of energy in a lattice, one must therefore perform a statistical analysis of the outcome of many collisions [10]. Figure 3 illustrates the results of such a study obtained from 200 collisions of a stationary "big breather" and "small breathers" with a gaussian distribution of initial amplitudes, positions, and initial velocities [10]. The energy exchange in each collision is measured relatively to the initial energy of the small breather by

$$\Delta H_1 = \frac{E_{\rm big}(\text{after}) - E_{\rm big}(\text{before})}{E_{\rm small}(\text{before})} \ . \tag{8}$$

Then an histogram giving the probabilities of the various values of the energy exchange is built. Similarly the displacement Δn_1 of the big breather in the collision can also be measured. These calculations confirm the observation made of Fig. 2: *collisions tend to favor big breathers.* On average the energy transfer goes from the small amplitude excitations to the large amplitude ones. This is shown by the probability distribution of ΔH_1 on Fig. 3 which is clearly biased toward a positive value. This provides a mechanism by which the small amplitude breathers that emerge from modulational instability can grow and give rise to excitations with a very high energy density. Moreover this mechanism for growth has been found to be very robust and weakly dependent on the on-site nonlinear potential or the presence of thermal noise [10].

2.3 Localization of thermal fluctuations.

Up to know we have assumed that energy was introduced in the lattice in a coherent way, under the form of a plane wave, eventually slightly modulated. Although it is conceivable to excite a crystal coherently, in many cases the

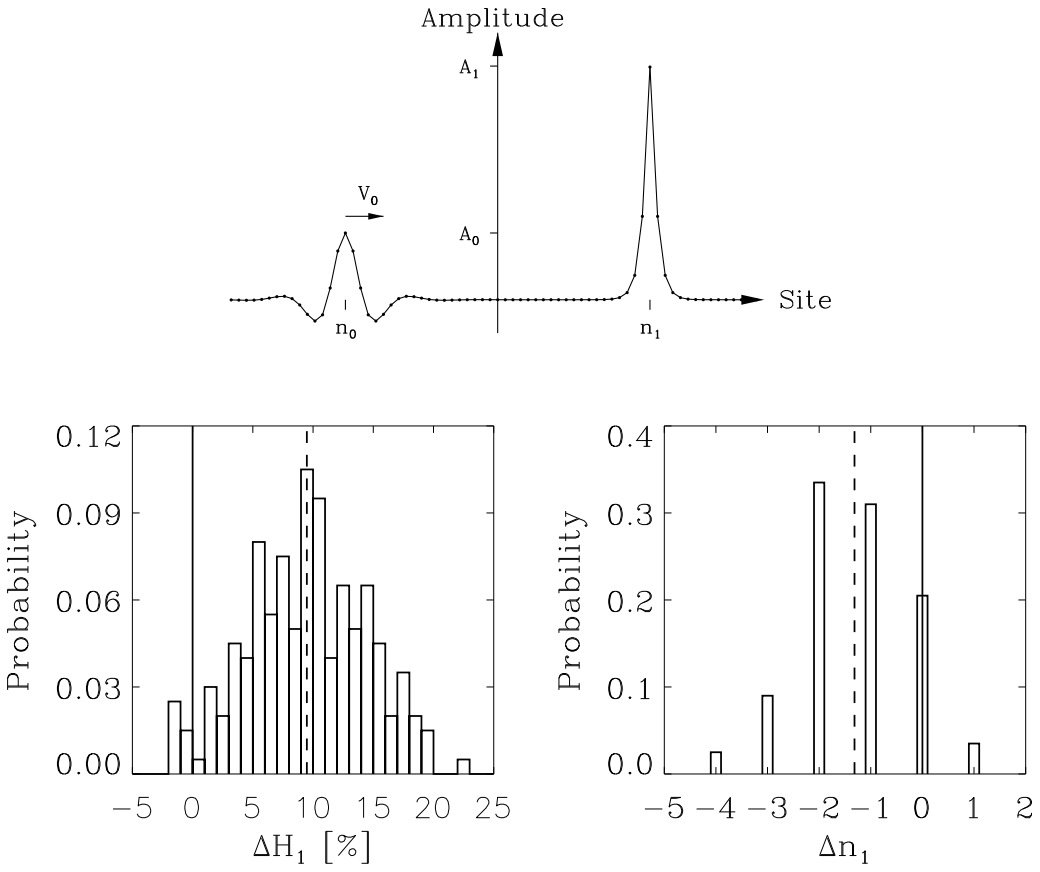

Fig. 3. Upper figure: typical initial condition for the study of discrete breather collisions. Lower figure: Probability distribution of (left) the energy transfer to the big breather ΔH_1 and (right) its displacement Δn_1 found from a set of 200 simulations. The dashed lines indicate the mean values $\overline{\Delta H_1} = 9\%$ and $\overline{\Delta n_1} = -1.3$.

energy will be provided as thermal fluctuations. Numerical simulations show that breathers are also observed in this case. This was in particular checked for a lattice of coupled Morse oscillators which is a very simple model of the dynamics of base pairs in DNA [11], but, as discussed below this is not specific to this model.

3 Discrete breathers in complex systems.

The results of Sec. 2 show that discrete breathers can exist et can be easily generated in a simple one-dimensional lattice of coupled nonlinear oscillators. Although such a lattice may be a crude model of some physical systems, real systems are often much more complicated. They may involve more than one

degree of freedom per site, or more than one spatial dimension. Therefore, in order to conclude on the possible relevance of localized modes in physics, we must consider systems that are more complex than the lattice studied in Sec. 2. This section considers two kinds of generalizations.

3.1 Intrinsic localized modes in a multicomponent nonlinear lattice.

Let us consider first a generalization of the simple DNA model mentioned above. We consider a two-chain system with an hamiltonian given in dimensionless form by

$$H = \sum_n \frac{1}{2}\Big[\left(\frac{dU_n}{dt}\right)^2 + \left(\frac{dV_n}{dt}\right)^2 \Big] + \frac{1}{2}K(U_{n+1}-U_n)^2 + \frac{1}{2}K'(V_{n+1}-V_n)^2 + \Big[\exp[-(U_n-V_n)]-1\Big]^2 . \tag{9}$$

The two degrees of freedom per cell, U_n and V_n describe the transverse displacements of the two bases belonging to the base pair labeled by index n in the DNA molecule. The coupling of two nucleotides along the same strand is assumed to be harmonic, with coupling constants K and K'. The interaction between the two bases in a pair is modeled by a Morse potential which represents the hydrogen bonds coupling the bases as well as the repulsive interaction between the phosphate groups. It is interesting to consider the new variables

$$X_n = \frac{U_n + V_n}{\sqrt{2}} \qquad Y_n = \frac{U_n - V_n}{\sqrt{2}} , \tag{10}$$

where X_n describes the acoustic motions of the two-chain system while Y_n corresponds to the stretching of the bond connecting the two strings.

The existence of discrete breathers in such a system is no longer obvious because the spectrum of the linear phonon modes includes two bands, corresponding to acoustic and optical modes as shown in Fig. 4. As a result, the breathers, which have a frequency below the optical phonon band, could be in resonance with acoustic phonons. The proof of existence of discrete breathers as exact solutions can however be extended to the two-chain system [12]. As expected exact breathers exist only in the gap between the optical and acoustic bands. This could be a problem for a real system with several degrees of freedom per unit cell because the various phonon bands could overlap and close completely the gap. This may also happen for the two-chain model when the coupling along the chains increases. However, numerical simulations show that, even when it resonates with the acoustic band, a breather can have a

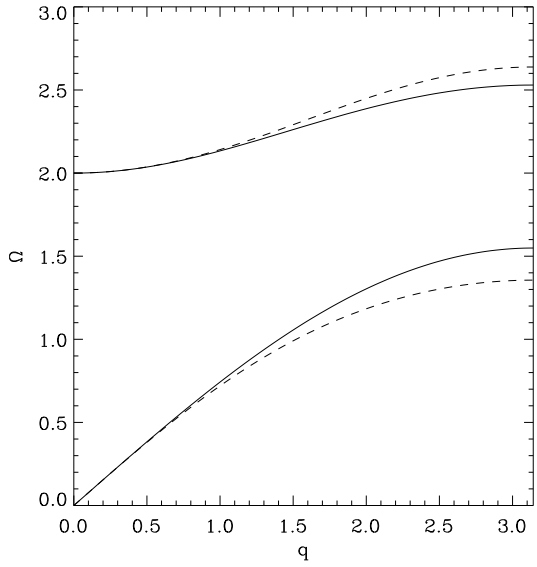

Fig. 4. Dispersion curves for the two chain model. (a) $K-+=(K+K')/2=0.6$ and $K_-=(K-K')/2=0$ (full lines), (b) $K-+=(K+K')/2=0.6$ and $K_-=(K-K')/2=0.4$ (dashed lines)

very long lifetime [13]. This indicates that the coupling between a highly localized mode and extended phonons is weak. But, more importantly, the growth of breathers through collisions with smaller excitations is still effective in a complex lattice. This has two consequences. First, collisions can prevent the decay of an unstable breather by feeding-in some energy. This is illustrated in Fig. 5. Second, the spontaneous formation of breathers from thermal fluctuations is possible in a multicomponent lattice as it is in a simple lattice. This is shown in Fig. 6 which shows the acoustic X displacements and the optical Y displacements in the two-chain model in contact with a thermal bath. As shown by hamiltonian (9), the nonlinearity appears only in the stretching motion $Y=U-V$. Figure 6 shows that the acoustic displacements do not show localization. They are simply dominated by the lowest energy mode which is the bending of the chain with a wavelength equal to the system size. On the contrary the stretching Y shows large amplitude localized modes that may survive for hundreds of phonon periods, although at the high temperature shown in Fig. 6 their lifetime is shorter.

3.2 Formation of breathers from thermal fluctuations in a two-dimensional lattice.

The proof of existence of discrete breathers is also valid in more than one spatial dimension, so that they could exist as surface modes (in two dimensions) or as volume modes (in three dimensions). However in theses cases it is not

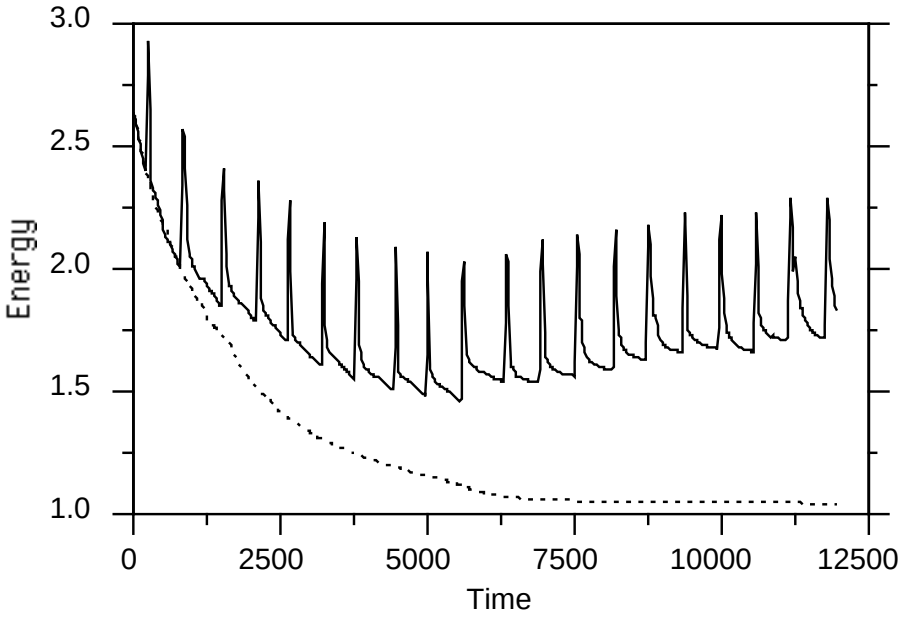

Fig. 5. Time evolution of the energy of a weakly unstable big breather undergoing multiple collisions with small breathers. $K = 0.7$, $K' = 0.5$. The big breather has frequency $\omega_b = 1.4$. The full line shows the energy of the big breather undergoing multiple collisions with incoming small breathers. The dotted line shows the time evolution of the energy of the same big breather without the collisions. It slowly decays in amplitude and increases in frequency until it reaches a stable state with a lower energy when its frequency has raised above the acoustic phonon band.

clear that breathers can be formed from thermal fluctuations because it has been recently shown that they can only exist above a given energy threshold [14]. This is a fundamental difference with the one-dimensional case where breathers can exist even in the limit of vanishing energy. In this limit they tend toward phonon modes. Therefore it was important to test the possible spontaneous formation of breathers in more than one spatial dimension. This has been done for a two dimensional lattice of Morse oscillators with hamiltonian

$$H = \sum_{l,m} \frac{1}{2}\left(\frac{du_{l,m}}{dt}\right)^2 + \frac{1}{2}K[(u_{l,m+1} - u_{l,m})^2 + (u_{l+1,m} - u_{l,m})^2] + \frac{1}{2}\omega_0^2\left(e^{-u_{l,m}} - 1\right)^2 \quad . \tag{11}$$

The indices l and m denote the sites along the x and y axes. The displacement at each site is characterized by a scalar variable $u_{l,m}$, and the harmonic coupling along the x and y axes is isotropic. The time evolution of this model system in contact with a thermal bath has been simulated with the Nose method [15], with periodic boundary conditions, $N_x = 32$ cells along the x axis, $N_y = 16$ cells along the y axis. Figure 7 shows a typical sample of the time evolution of the system for $\omega_0^2 = 16$, $K = 0.05$. The evolution of a

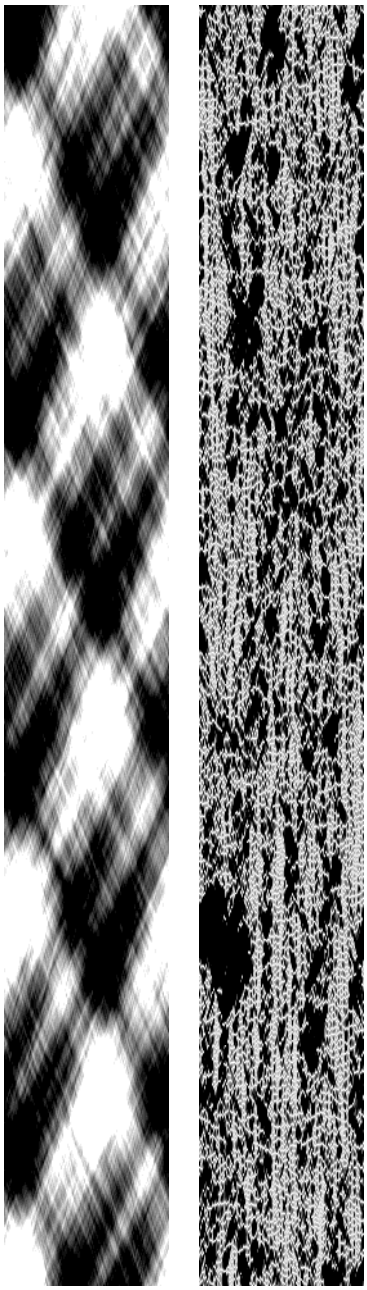

Fig. 6. Thermal generation of localized excitations in the two-chain model. The coupling constants are $K = 0.3$, $K' = 0.1$. The temperature is $T = 0.8$ in energy units. The grey scale figures show the X and Y displacements of the different lattice sites versus time. The horizontal axis extends along the lattice which has 128 cells with periodic boundary conditions. The vertical axis is the time axis. It extends over 1000 time units, i.e. 500 periods of the lowest optical mode. Left: X_n (acoustic displacements); grey scale from $X < -10$ (white) to $X > +10$ (black). Right: Y_n (optical displacements); grey scale from $Y < -0.5$ (white) to $Y > +5$ (black).

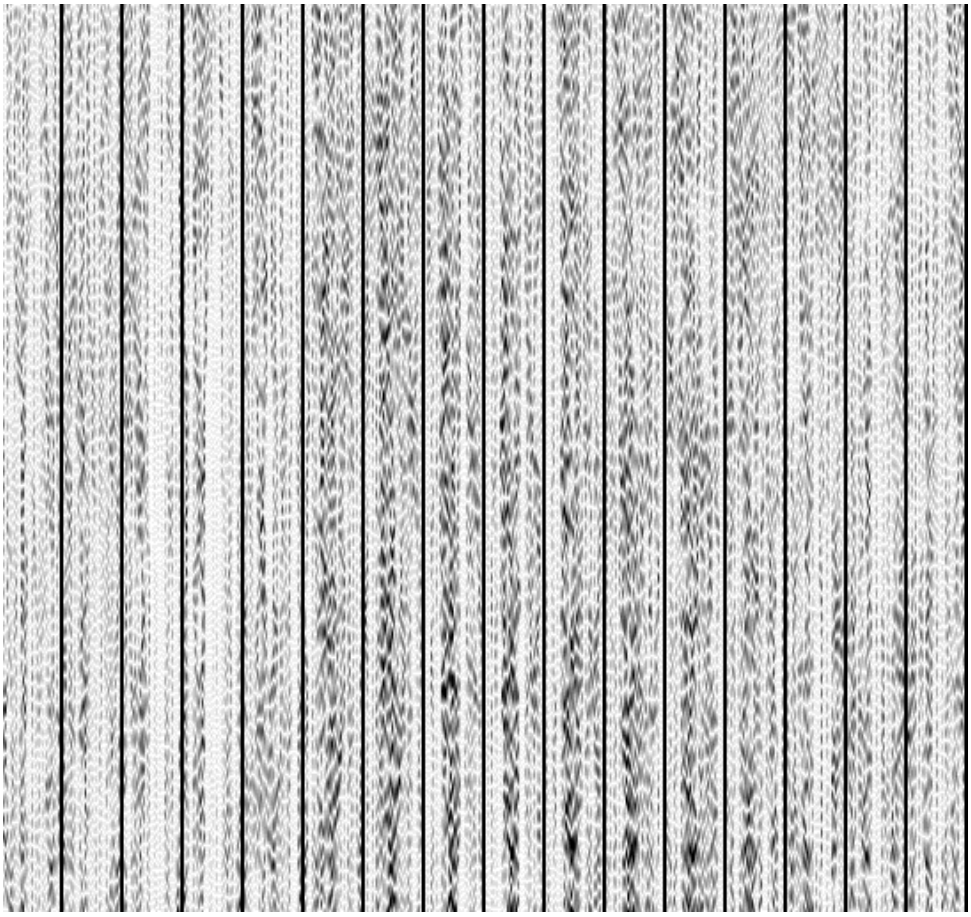

Fig. 7. Time evolution of the displacements of a thermalized lattice of Morse oscillators along 1000 periods $T_0 = 2\pi/\omega_0$. The lattice has $N_x \times N_y = 32 \times 16$ cells. Each of the 16 columns of the figure (between two black vertical lines) shows the time evolution of a row in the lattice. The grey scale shows the amplitude of the displacements from $u = -1$ (white) to $u = 15$ (black).

given row of the two-dimensional lattice is very similar to the evolution of a one-dimensional lattice of Morse oscillators. It shows the existence of localized breathing excitations that survive for hundreds of phonon periods. The comparison of the evolution of neighboring rows shows that these modes are localized in both spatial directions. The spontaneous localization of thermal energy in a nonlinear lattice appears clearly when one compares the time evolution of the lattice of Morse oscillators with the evolution of a similar lattice of harmonic oscillators on Fig. 8. This figure illustrates one example of a large amplitude mode, situated roughly at the center of the nonlinear lattice, which is shown for about 100 phonon periods, whereas the harmonic lattice shows a uniform pattern of displacements.

Although they are restricted to one particular type of nonlinear lattice (lattice of Morse oscillators) these numerical simulations show that intrinsic localized modes can emerge from thermal fluctuations even in more that one spatial

dimension, in spite of the energy threshold that has been found for the discrete breathers in this case [14]. The only significant difference with the one-dimensional case is the value of the coupling constant K that we have used to observe a similar self localization of thermal energy. For the same on-site potential characterized by $\omega_0^2 = 4$, the simulations have been performed with $K = 0.1$ in one spatial dimension, and $K = 0.05$ in the two-dimensional case. In fact this difference is understandable because in the two dimensional case, when an atom is displaced with respect to its equilibrium position, it is recalled to equilibrium by the forces exerted in the x and y directions. Thus, dividing K by 2 amounts to choosing the same restoring force as in the one-dimensional case. This shows that the dimension is not a critical factor for the formation of discrete breathers as long as the system stays sufficiently discrete, i.e. as long as the total coupling with the neighbors is sufficiently small compared to the force coming from the on-site potential.

4 Observing discrete breathers in experiments.

Spectroscopic experiments, such a Raman scattering, or inelastic neutron scattering experiments can probe the dynamical structure factor $S(q, \omega)$ which is the Fourier transform of the space–time correlation function of the atomic displacements $S(q, \omega) = \mathcal{F}\langle u_n(t)u_0(0)\rangle$. In order to determine how breathers would appear in such experiments, we have calculated the structure factor for a thermalized one-dimensional lattice of Morse oscillators. Figure 9 shows typical results. The grey scale picture clearly shows the presence of breathers and the structure factor exhibits three characteristic features. The first one is a broad band that covers the full range of q values, i.e. corresponds to non-localized modes, and follows the general shape of the phonon band (shown as a dash-dot line on the contour plot), but with lower frequencies. This band corresponds to anharmonic phonons. In the Morse potential the frequency of the vibration decays when the amplitude increases. This is why the anharmonic phonons are situated below the harmonic band. The second noticeable feature is a small peak, with a frequency immediately below the phonon band, and limited to small wavevectors. It is essentially visible in the bottom left diagram of Fig. 9. The third feature of the structure factor is the very strong low frequency component, which has a large peak that dominates the structure factor at small wavevectors, but extends however over the whole Brillouin zone, as shown in the contour plot. In order to understand the origin of the second and third feature, it is useful to start from the approximate breather solution provided by the multiple scale expansion. As the Morse potential contains a cubic contribution, in the semi–discrete approximation, one looks for a solution of the form

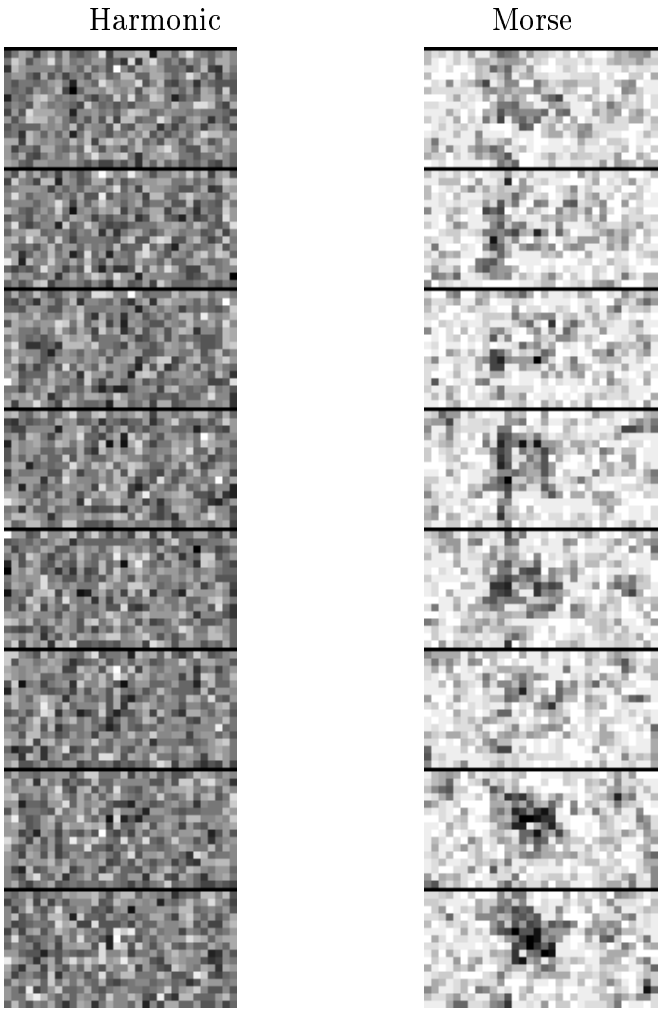

Fig. 8. Snapshots of the spatial distributions of the displacements, shown with a grey scale, in thermalized two-dimensional lattice of harmonically coupled oscillators. Model parameters: $N_x \times N_y = 32 \times 16$ cells, $K = 0.05$, $\omega_0^2 = 4$. The snapshots, separated by horizontal black lines, have been recorded at a time interval $\Delta t = 40$, which must be compared to the period $T_0 = \pi$ of the bottom of the phonon band. Left: lattice of harmonic oscillators; grey scale range $[-2, 2]$. Right: lattice of Morse oscillators; grey scale range $[-1, 15]$.

$$u_n(t) = \epsilon \left[F_{1,n} e^{i\theta_n} + c.c. \right] + \epsilon^2 \left[F_{0,n} + F_{2,n} e^{2i\theta_n} + c.c. \right] + O(\epsilon^3) \tag{12}$$

with $\theta_n = qn - \omega t$, where ω and q are related by the dispersion relation of the discrete lattice. Introducing this expression into the equations of motion one gets a nonlinear Schrödinger equation for F_1 which leads to the solution $u_n(t)$ under the form

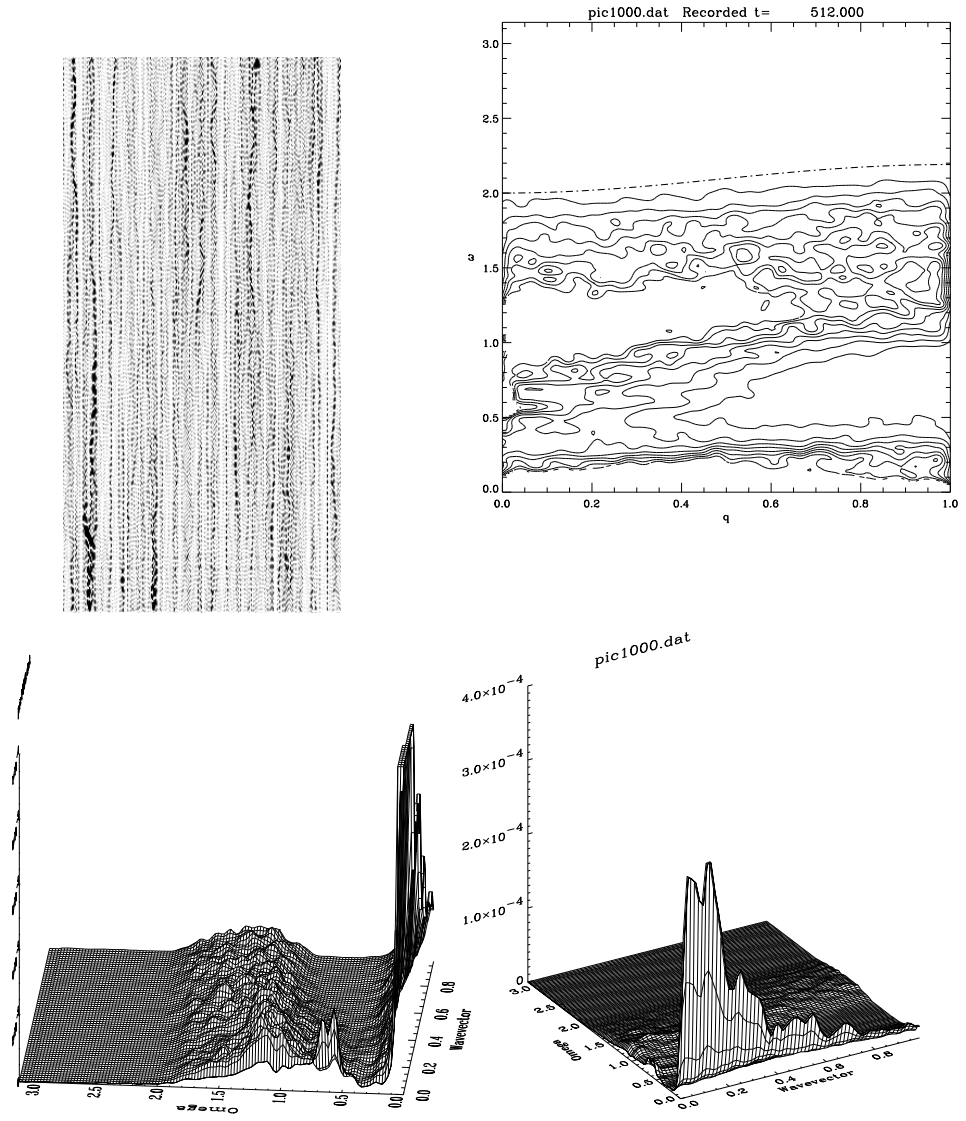

Fig. 9. Structure factor $S(q,\omega)$ for a thermalized one-dimensional lattice of Morse oscillators ($N = 256$ cells, $K = 0.2$, $\omega_0^2 = 4$, temperature in energy units $T = 0.8$) . The top left figure shows the corresponding displacements $u_n(t)$ with a grey scale. the top right figure shows a contour plot of $S(q,\omega)$. The dash-dot lines shows the theoretical phonon dispersion curve. The two bottom figures show the surface $S(q,\omega)$ from two different point of view.

$$
\begin{aligned}
u_n(t) = \; & 2\epsilon A \mathrm{sech}[\epsilon(n - V_e t)/L_e] \cos(\Theta n - \omega_b t) \\
& + 2\epsilon^2 A^2 \mathrm{sech}^2[\epsilon(n - V_e t)/L_e] \\
& \times \left\{ 1 - \frac{1}{3 + (16/\omega_0^2)\sin^4(\frac{q}{2})} \cos[2(\Theta n - \omega_b t)] \right\} ,
\end{aligned} \tag{13}
$$

where A determines the amplitude of the solution, V_e is the velocity of the envelope, $\omega_b < \omega_0$ is the breather frequency and L_e determines its width (ω_b

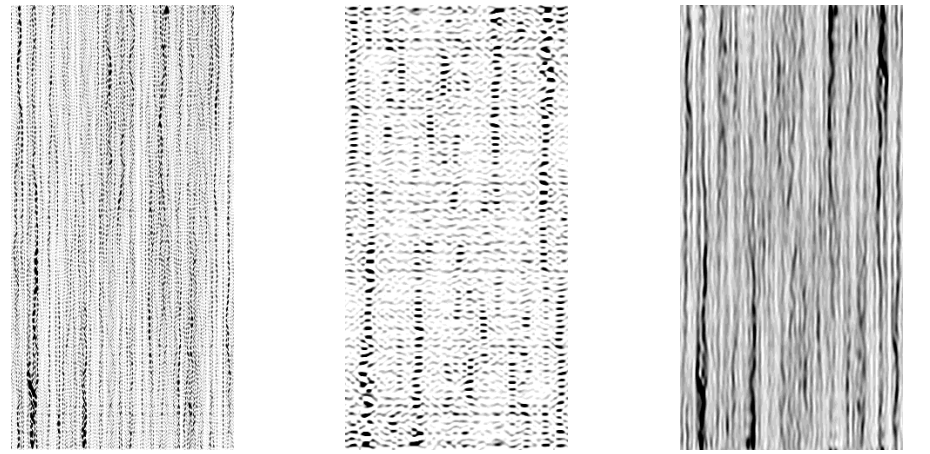

No filter	$-0.2 < q < 0.2$	$-0.4 < q < 0.4$
	$0.35 < \omega < 0.95$	$0 < \omega < 0.35$
$\langle u \rangle = 0.49$	$\langle u \rangle = 0.0$	$\langle u \rangle = 0.49$

Fig. 10. Effect of a filter in ω and q on the displacement pattern of the thermalized chain of Morse oscillators. Left: original displacement pattern. Middle: pattern restricted to the frequency components $0.35 < \omega < 0.95$ and wavevectors $-0.2 < q < 0.2$. Right: pattern restricted to the frequency components $0 < \omega < 0.35$ and wavevectors $-0.4 < q < 0.4$. The mean value of the displacements is given for each pattern.

and L_e can be expressed in terms of the breather amplitude and velocity, and the model parameters [13], but their expressions are not useful for the present discussion) The second and third features of the structure factor can be understood in terms of this approximate solution. The low frequency central peak (third feature) is associated to $F_{0,n}(t)$ while the breather frequency ω_b which appears in the cosine factor of $F_{1,n}(t)$ is responsible of the small peak of the second feature. This interpretation can be checked numerically by filtering some components in ω and q in the Fourier transform of $u_n(t)$ and plotting the backward Fourier transform of the filtered data. The results if shown in Fig. 10. The left figure shows the full displacement pattern recorded for 512 time units. The middle picture shows the pattern obtained by Fourier transforming the full pattern and then selecting only a small frequency domain below the phonon band ($0.35 < \omega < 0.95$) and a small range of wavevectors around $q = 0$ ($-0.2 < q < 0.2$). This region in the spectrum corresponds to the small peak denoted as the "second feature" in the structure factor. The picture shows clearly large oscillations situated at the positions of the breathers, but, the mean value of the displacements is now equal to 0. This is consistent with the selection of the F_1 term in the approximate solution (12). The right picture shows the pattern obtained by retaining only the low frequency components $0 < \omega < 0.35$ and a range of low wavevectors broader than previously ($-0.4 < q < 0.4$). It shows black lines at the positions of the

breather, without the fast oscillatory component due to the filtering, which is consistent with the selection of the F_2 component of the solution. There is however one component of the third feature of the structure factor which is not yet reproduced; it is the low frequency component at large wavevectors. This contribution is a two-phonon contribution coming from the u^2 term in the equation of motion. If one considers the sum of two phonon modes

$$u = U_1 e^{i(q_1 n - \omega_1 t)} + c.c. + U_2 e^{i(q_2 n - \omega_2 t)} + c.c. \ , \tag{14}$$

the square term gives factors of the form $\exp\left\{i[(q_1 - q_2)n - (\omega_1 - \omega_2)t]\right\}$ which contains low frequency contributions at all wavevectors, in a range that coincides very well with the part of the third feature of the structure factor which is not accounted for by the breathers.

This type of analysis allows us to assign the various features of the structure factor of a nonlinear lattice. It indicates that *the dominant feature is not at the breather frequency* but in the low frequency range and shows up as a broad central peak. This calls for two remarks. First it shows the limitation of the multiple scale analysis because, in this approach, the low frequency component F_2 is a second order term, while F_1 is first order. In the thermalized lattice we find that the "second order" component plays in fact a larger role in the structure factor than the "first order" one. Second the main signature of the breathers in the structure factor is not favorable for their experimental detection because, in experiments performed on a real material, there are many other possible contributions to the central peak, beyond the breathers, in particular the static scattering by defects broadened by the limited instrumental resolution. This is why the central peak in ferroelectrics lead to such debates for instance. One could think of looking for systems in which this dominant central peak feature would be absent in order to allow a simpler observation of features that are truly characteristic of breathers. This would be the case in systems with a symmetric on-site potential, so that the equations do not contain a quadratic term. Let us consider for instance a lattice of oscillators with the on-site potential

$$V(u) = \frac{1}{2}\omega_0^2 \left[e^{-|u|} - 1\right]^2 . \tag{15}$$

Figure 11 shows the structure factor of such a system in contact with a thermal bath with the same parameters as for the Morse lattice discussed above. As expected the structure factor contains neither the central peak nor the two phonon contribution, i.e. the third feature of the structure factor of the Morse lattice has vanished. This does not mean however that the breathers would be easier to detect in a experiment because the breather peak (second feature of the structure factor) is almost mixed with the phonon band broaden

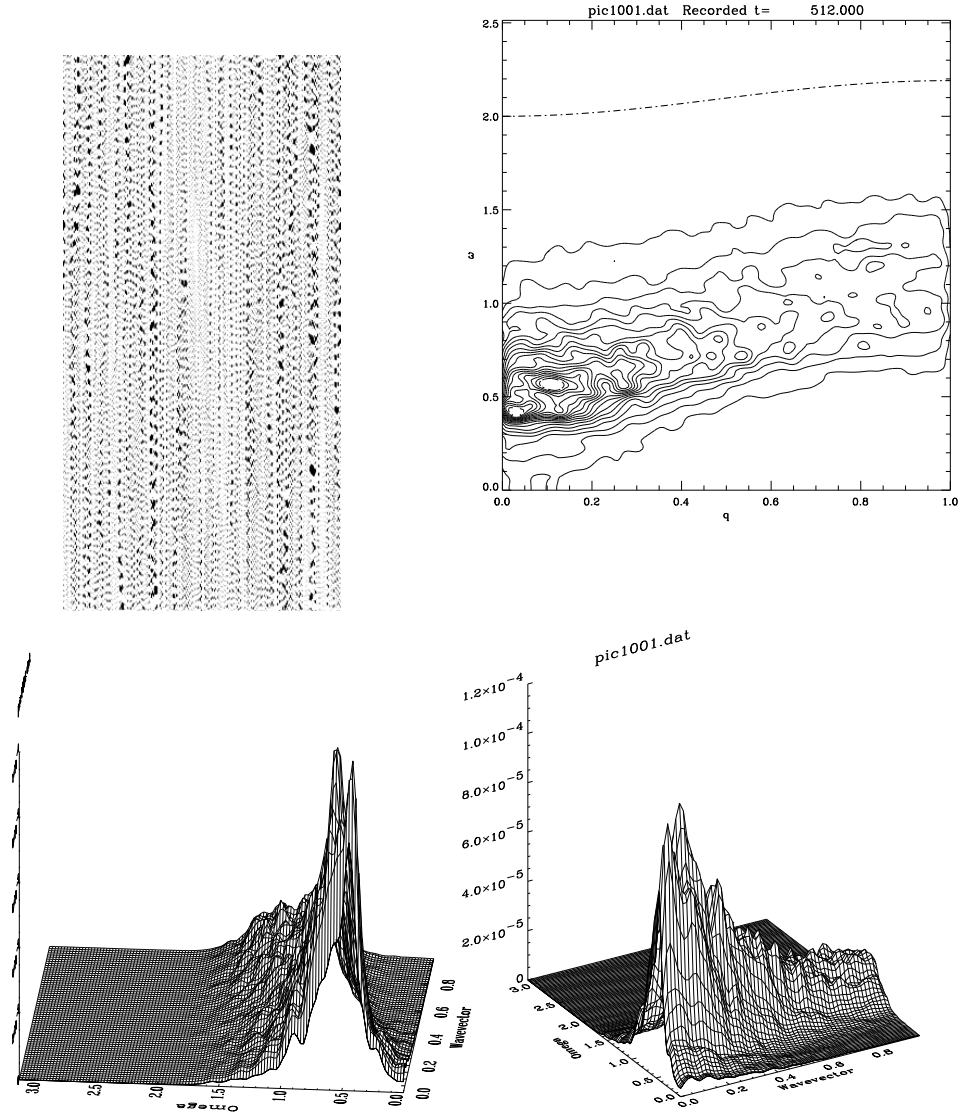

Fig. 11. Structure factor $S(q,\omega)$ for a thermalized one-dimensional lattice of oscillators with a symmetric on-site potential given by Eq. (15) ($N = 256$ cells, $K = 0.2$, $\omega_0^2 = 4$, temperature in energy units $T = 0.8$) . The top left figure shows the corresponding displacements $u_n(t)$ with a grey scale. the top right figure shows a contour plot of $S(q,\omega)$. The dash-dot lines shows the theoretical phonon dispersion curve. The two bottom figures show the surface $S(q,\omega)$ from two different point of view.

by the nonlinearity. This is because for a symmetric potential the nonlinearity appears at a higher order than for an odd potential so that the drop in frequency due to the large amplitude motion within the breathers is smaller. In the structure factor of Fig. 11 the presence of the breathers is essentially attested by the fact that the broad phonon band has a shoulder on the low frequency which decays when the wavevector q increases.

5 Conclusion.

The analysis of the pathways to energy localization in a lattice of coupled nonlinear oscillators shows that the formation of intrinsic localized modes is possible from a coherent energy input corresponding to a plane wave excitation of the lattice. It proceeds in two steps. First the modulational instability of the wave splits it into wavepackets which are small breathers. Then the interaction of these breathers tend to favor the largest excitations which grow at the expenses of the other. This process saturates when the breathers, that get narrower as they grow in amplitude, are so narrow that they are trapped by lattice discreteness and no longer move in the lattice. The formation of discrete breathers can also occur from thermal fluctuations. These mechanisms for the generation of highly localized modes, which had been initially found for simple one-dimensional lattices, have been shown to be valid in a much larger variety of systems, and in particular in a multicomponent one-dimensional lattice or a two-dimensional lattice. The possibility to form breathers from thermal fluctuations in various nonlinear lattice strongly suggests that they could exist in many physical systems.

The direct observation of discrete breathers seems however difficult. One could expect to detect them in the structure factor associated to atomic motions, which can be probed by experiments such as inelastic neutron scattering or Raman spectroscopy. However, in system with an on-site potential of odd symmetry, the dominant contribution of the breathers to the structure factor is a broad central peak which might be difficult to distinguish from a central peak due to static scattering or to slowly moving domain walls. If one considers systems with even on-site potential, the central peak is no longer present but the peak at the breather frequency is not well separated from the band of anharmonic phonons because nonlinearity occurs at a higher order.

This indicates that it may be difficult to find the track of breathers in *equilibrium* properties such as the two-point correlations functions although the breathers break *temporarily* the equipartition of energy. This suggests that one should look at *non-equilibrium properties* and attempt to detect some indirect effects of breathers on the physical properties of a system. A recent work of Aubry and Tsironis has shown for instance the role of breathers to modify the relaxation rate of a lattice put into contact with a cold bath[16]. The case of DNA, for which the lattice of Morse oscillators is a crude model, the breathers correspond to large amplitude, temporary, openings of the base pairs. They could be the precursor of the thermal denaturation of DNA [11]. They are observed indirectly because the opening of a base pair corresponds to the breaking of the hydrogen bonds linking the bases. This leaves the hydrogen available for chemical reactions, and in particular for exchange with deuterium when DNA is in deuterated water [17]. The case of DNA gives some hints on a pos-

sible role of intrinsic localized modes in biological molecules. Theses molecules are highly deformable and undergo large amplitude nonlinear displacements, so that the formation of localized modes from thermal fluctuations seems likely to occur, especially because biological molecules combine two possible sources of localization, nonlinearity and disorder. While, as discussed above, localized modes my be hard to detect by the observation of the equilibrium properties of the molecule, they could have a dramatic effect if these anomalously large fluctuations are at the origin of a chemical reaction. The possible role of intrinsic localized modes on the kinetic of biological reactions is currently under investigation [18].

References

[1] S. Takeno, K. Kisoda and A.J. Sievers, Progr. Theor. Phys. Supplement No. 94, 242-269 (1988), K. Hori and S. Takeno, J. Phys. Soc. of Japan **61**, 2186 (1992)

[2] S. Flach *Conditions on the existence of localized excitations in nonlinear discrete systems.* Phys. Rev. E **50**, 3134 (1994)

[3] S. Flach, C.R. Willis and E. Olbrich, *Integrability and localized excitations in nonlinear discrete systems.* Phys. Rev. E **49** 836 (1994)

[4] R.S. MacKay and S. Aubry, Nonlinearity **7** 1623 (1994)

[5] S. Aubry, *Breathers in nonlinear lattices: existence, linear stability and quantization,* to be published in Physica D.

[6] Yu. S. Kivshar and M. Peyrard Phys. Rev. A **46** 3198 (1992)

[7] I. Daumont, T. Dauxois and M. Peyrard, Nonlinearity **10**, 617 (1997)

[8] S. Flach and C.R. Willis, Phys. Rev. Lett. **72**, 1777 (1994)

[9] T. Dauxois, private communication.

[10] O. Band and M. Peyrard, Phys. Rev. E **53**, 4143 (1996)

[11] T. Dauxois, M. Peyrard and A.R. Bishop
Phys. Rev. E **47**, 684 (1993)

[12] S. Aubry, unpublished.

[13] K. Forinash, T. Cretegny, M. Peyrard, Phys. Rev. E **55**, 4740 (1997).

[14] S. Flach, K. Kladko and R.S. MackKay, Phys. Rev. Letters **78**, 1207 (1997)

[15] S. Nose, J. Chem. Phys. **81**, 511 (1984)

[16] G. P. Tsironis and S. Aubry, Phys. Rev. Lett. **77**, 5225 (1996)

[17] M. Gueron, M. Kochoyan and J-L Leroy Nature**328**, 89 (1987)

[18] J. Farago and M. Peyrard, unpublished.